ASEC 2025 Conference
The 6th International Electronic Conference on Applied Sciences
09–11 December 2025 | Online
MDPI

Electronic structures, optical and acoustic phonons, and electronic and thermal conductivities of cesium ytterbium chloride perovskite crystal

Atsushi Suzuki, Takeo Oku E-mail: suzuki@mat.usp.ac.jp
The University of Shiga Prefecture, Japan.

INTRODUCTION & PURPOSE

Introduction

Perovskite solar cell

- Control of crystal structure, mole ratio.
- V_{oc} > 1.0 V Si, E_g ≈ 1.6 eV,
- Conversion efficiency η ≈ Si, GaAs
- Wavelength (300 - 800 nm)
- Easy fabrication process by spin coating
- Easily decomposition in air atmosphere
- Subject: Stability

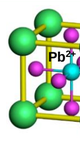

Perovskite crystal

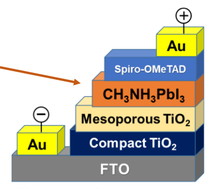

Perovskite solar cell

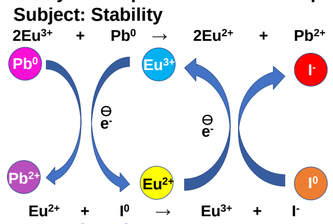

Eu^{3+}-Eu^{2+} Redox reaction

Wang et al., Science 363 (2019) 265–270.

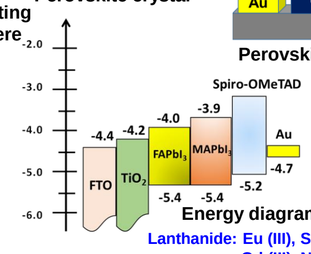

Energy diagram of solar cell

Lanthanide: Eu (III), Sm (III), Tb (III), Gd (Nd (III), Yb (II)

Fluorescence, wavelength conversion, Redox reaction ⇒ Improved Photo-voltaic properties and stability

Ln-doped $CsPbX_3$ crystal
Ln-double perovskite crystal
Subject: band gap expansion

A. Suzuki, T. Oku, Jpn. J. Appl. Phys. 57 (2018) 02CE04-1-7.
A. Suzuki, M. Oe, T. Oku, J. Electron. Mater. 50 (2021) 1980.
A. Suzuki, T. Oku, Heliyon 4 (2018) e00755-1-22.
A. Suzuki, T. Oku, Mater. Adv. 2 (2021) 2609-2616.
A. Suzuki, T. Oku, Jpn. J. Appl. Phys. 62 (2023) SK1006.

Purpose

Electronic structure, optical and thermal properties of lanthanide doped perovskite crystals was predicted for practical application in solar cell.

RESULTS & DISCUSSION

Characterization of perovskite crystal and stability

ions	Ionic radius (pm)
MA^+	217
FA^+	253
EA^+	274
GA^+	278
K^+	138
Cs^+	174
Pb^{2+}	119
Ce^{3+}	101
Nd^{3+}	98.3
Nd^{2+}	129
Gd^{3+}	93.8
Yb^{2+}	102
F^-	133
Cl^-	181
Br^-	196
I^-	220

Perovskite	Tolerance factor (t)
$CsNdCl_3$	0.810
$CsGdCl_3$	0.914
$CsYbCl_3$	0.887
$CsPbCl_3$	0.837

Lattice constant (Å)	
$CsNdCl_3$	4.911 [1)]
$CsGdCl_3$	5.605 [1)]
$CsYbCl_3$	5.605 [1)]
$CsPbCl_3$	5.672 [1)]

$$t = \frac{r_A + r_X}{\sqrt{2}(r_B + r_X)}$$

1) Optimized structures. ($Pm\bar{3}m$)
Exp. $CsPbCl_3$, 5.605 Å

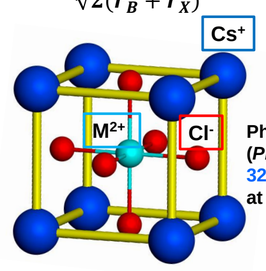

Lanthanide-doped perovskite crystal

J. Hutton *et al J. Phys. C: Solid State Phys.* **12** (1979) 5393.

Phase transition $CsPbCl_3$, cubic (*Pm3m*) - tetragonal (*P4/mbm*) at 325 K and - orthorhombic (*Pbnm*) at 316 K.

Ref. Y. He, et. al, *J. Am. Chem. Soc.* **143** (2021) 2068–2077.

Electron density distribution of $CsYbCl_3$

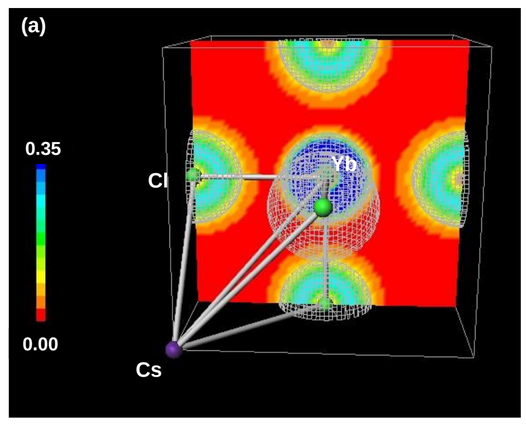

Yb^{2+}
6s, p orbital

5d orbital
anisotropy

4f^{14} orbital
occupancy

Cubic
a = 5.6050 Å
α = β = γ = 90°

Yb^{2+} 4f^{14}, 5d, 6s, p

Electron density distribution of s, p, d and f orbital at Yd ion

6s = 0.32,
6p = 0.26, p_z = 0.09, p_x = 0.09, p_y = 0.09,
5d = 0.25, d_{z2} = 0.09, d_{xz} = 0.02, d_{yz} = 0.02, d_{x2-y2} = 0.09, d_{xy} = 0.02,
4f = 13.93, f_{z3} = 1.99, f_{xz2} = 1.99, f_{yz2} = 1.99, $f_{zx2-zy2}$ = 1.99, f_{xyz} = 2.00, $f_{x3-3xy2}$ = 1.99, $f_{3yx2-y3}$ = 1.99

Electronic structure $CsYbCl_3$ cubic

Band structure

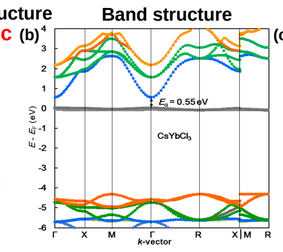

Effective mass ratio
m_e^* / m_0 = 0.01
m_h^* / m_0 = 0.17

PDOS

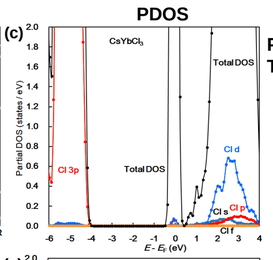

PDOS Cl$^-$ 3p
Total DOS

pDOS Yb^{+2}
6s, 5p, 5d, 4f

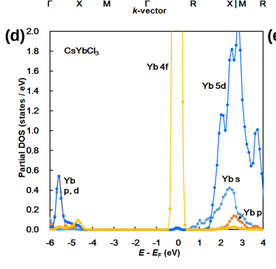

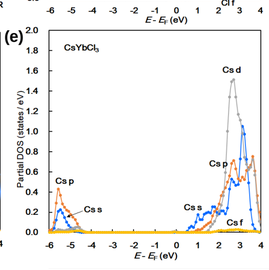

PDOS
Cs$^+$ 6s, 6p,

VB Yb 4f orbital
CB Yb 5d, 6s orbital, Cs 6s, p orbital
E_g = 0.55 eV Direct transition

Perovskite	Total Energy (eV/cell)	E_g (eV)
$CsNdCl_3$	-1443	1.5
$CsGdCl_3$	-1928	1.7
$CsYbCl_3$	-3434	0.6
$CsPbCl_3$	-3285	2.2

Dielectric function (Re, Im), Tauc plot $CsYbCl_3$

Real part
Re = 26.5

Imaginary part
Im = 32.2

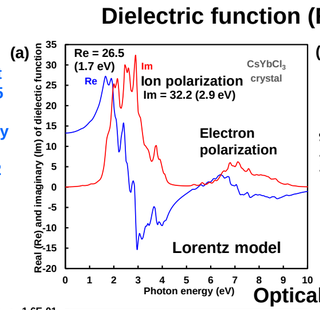

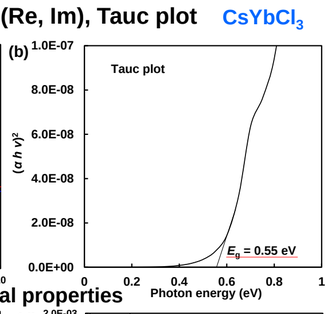

Optical properties

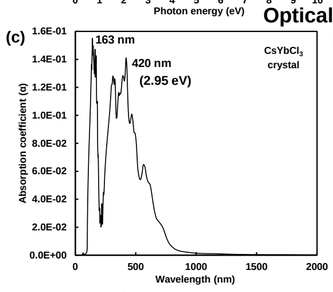

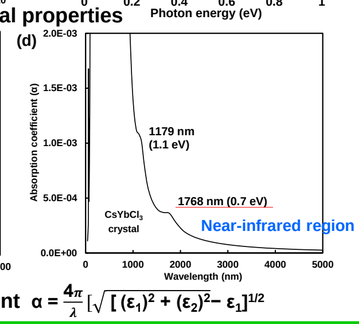

Absorption coefficient $\alpha = \frac{4\pi}{\lambda}\left[\sqrt{\left[(\varepsilon_1)^2 + (\varepsilon_2)^2 - \varepsilon_1\right]}\right]^{1/2}$

Electronic and thermal conductivity of $CsYbCl_3$ cubic

Boltzmann transport equation (BoltzTraP)

Relaxation-time-appro-ximated electrical con-ductivity (δ / τ) (300 K)

δ / τ = 3.2 ×10^{20} [/ Ω m s]
(E – E_F = 1.8 eV) (300 K)

δ / τ = 2.8 ×10^{20} [/ Ω m s]
(E – E_F = -0.19 eV) (300 K)

Electronic conductivity

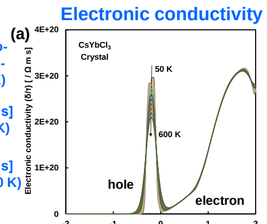

Temp. dependence

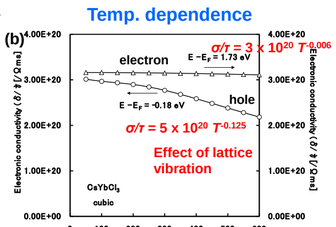

Seebeck coefficient

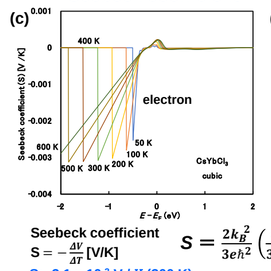

Seebeck coefficient
$S = -\frac{\Delta V}{\Delta T}$ [V/K]
S: -3.1 x 10^{-3} V / K (300 K)
N-type semiconductor

Thermal conductivity

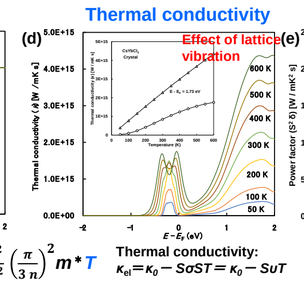

Thermal conductivity:
$S = \frac{2k_B^2}{3e\hbar^2}\left(\frac{\pi}{3n}\right)^2 m^* T$
$\kappa = \kappa_{el} + \kappa_{ph} = \kappa_0 - S\sigma ST = \kappa_0 - SuT$
κ_{el} : 2.2 x 10^{15} W / m K s (300 K)

Power factor

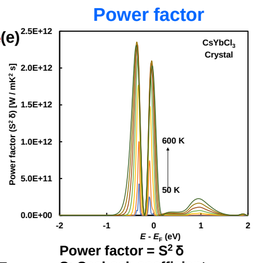

Power factor = S^2 δ
S: Seebeck coefficient
δ: Electrical conductivity
PF: 2.2 x 10^{12} W / m K^2 s (300 K)

A. Suzuki, T. Oku, Comput. Condens. Matter. 42 (2025) e01008

Electron density distribution of $CsYbCl_3$

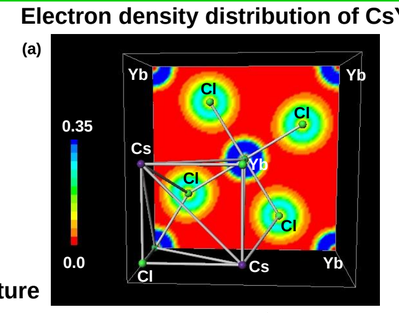

$CsYbCl_3$ crystal
tetragonal

a = 7.9682 Å
b = 7.9682 Å
c = 5.8110 Å
α = β = γ = 90°

Band structure

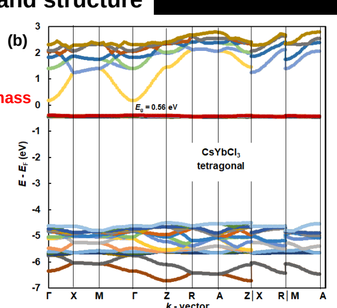

Effective mass
m_e^* = 0.01
m_h^* = 1.17

PDOS

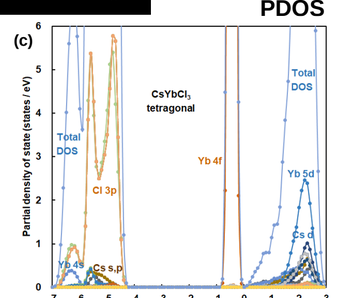

Dielectric function (Re, Im), Tauc plot $CsYbCl_3$ crystal (tetragonal)

Real part
Re = 28.9

Imaginary part
Im = 40.9

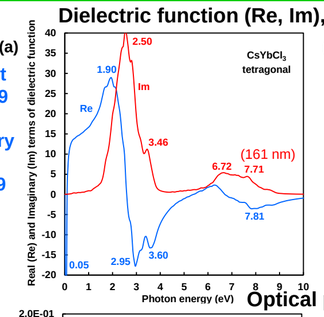

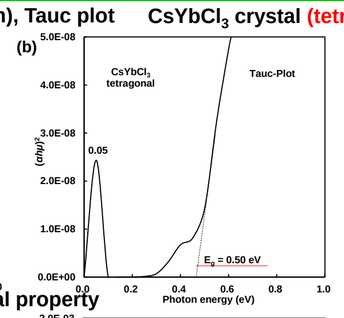

Optical property

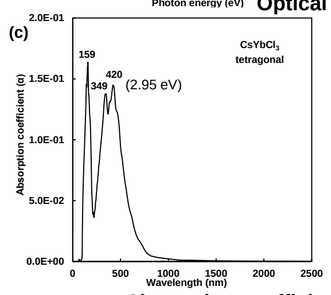

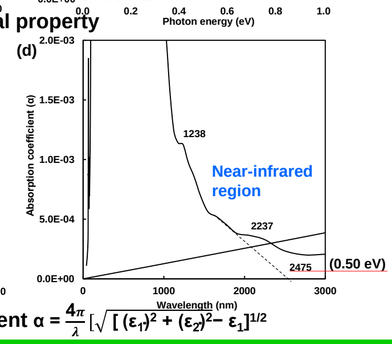

Absorption coefficient $\alpha = \frac{4\pi}{\lambda}\left[\sqrt{\left[(\varepsilon_1)^2 + (\varepsilon_2)^2 - \varepsilon_1\right]}\right]^{1/2}$

Electronic and thermal conductivity of $CsYbCl_3$ tetragonal

Boltzmann transport equation (BoltzTraP)

Relaxation-time-appro-ximated electrical con-ductivity (δ / τ) (300 K)

δ / τ = 1.1 ×10^{20} [/ Ω m s]
(Electron) (300 K)

Electronic conductivity

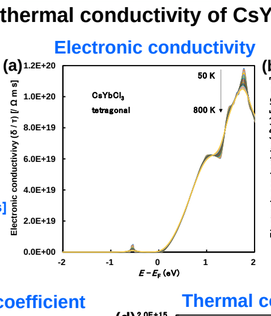

Temp. dependence

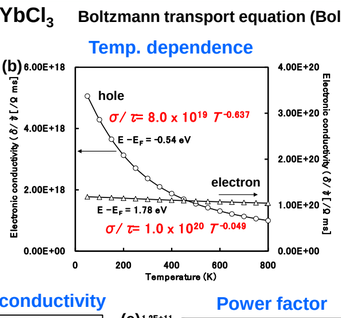

Seebeck coefficient

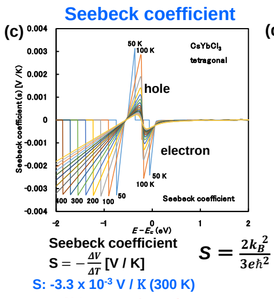

Seebeck coefficient
$S = -\frac{\Delta V}{\Delta T}$ [V / K]
S: -3.3 x 10^{-3} V / K (300 K)
N-type semi-conductor

Thermal conductivity

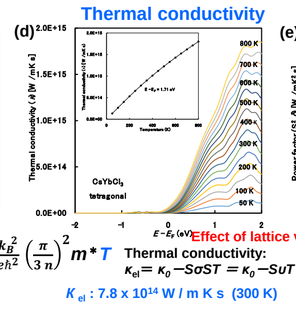

Effect of lattice vibrations

Thermal conductivity:
$S = \frac{2k_B^2}{3e\hbar^2}\left(\frac{\pi}{3n}\right)^2 m^* T$
$\kappa = \kappa_{el} + \kappa_{ph} = \kappa_0 - S\sigma ST = \kappa_0 - SuT$
κ_{el} : 7.8 x 10^{14} W / m K s (300 K)

Power factor

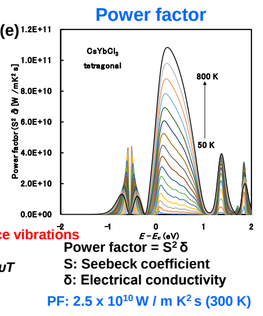

Power factor = S^2 δ
S: Seebeck coefficient
δ: Electrical conductivity
PF: 2.5 x 10^{10} W / m K^2 s (300 K)

Phonon band and phonon DOS

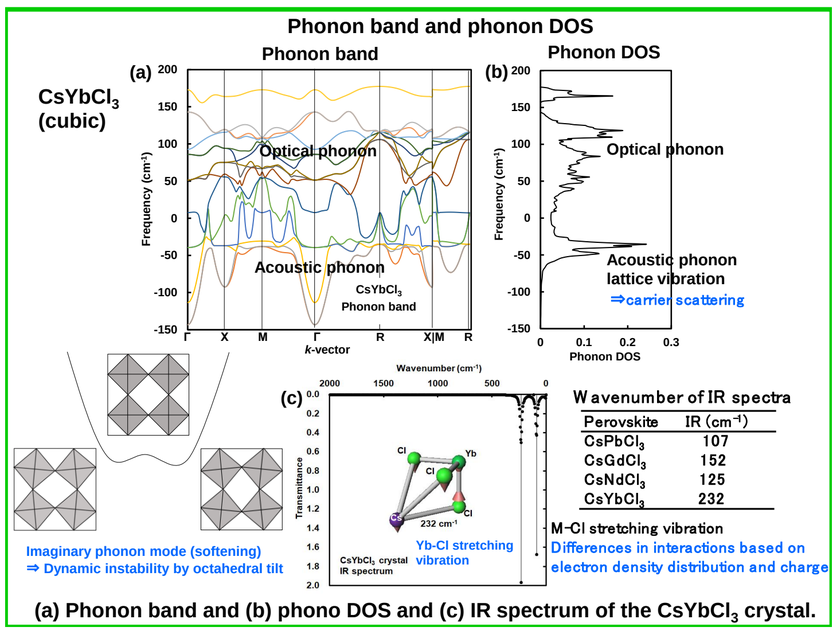

Wavenumber of IR spectra

Perovskite	IR (cm^{-1})
$CsPbCl_3$	107
$CsGdCl_3$	152
$CsNdCl_3$	125
$CsYbCl_3$	232

M-Cl stretching vibration
Differences in interactions based on electron density distribution and charge

(a) Phonon band and (b) phono DOS and (c) IR spectrum of the $CsYbCl_3$ crystal.

IR / Raman spectra

$CsYbCl_3$ (tetragonal)

IR spectrum

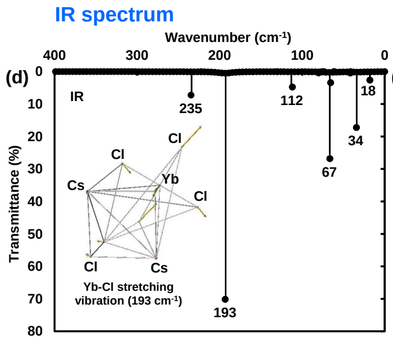

Raman spectrum

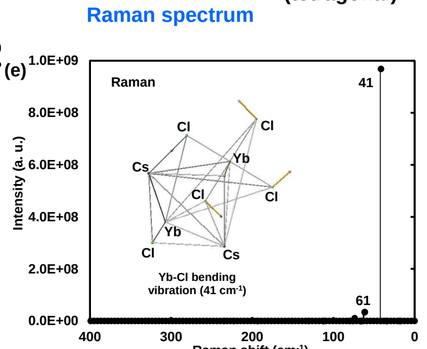

Yb-Cl stretching vibration

$CsYbCl_3$	IR (cm^{-1})
cubic	232
Tetragonal	193

Effect of crystal structure:
Distortion of the crystal structure,
Inter-bond interactions,
electron density distribution and charge

CONCLUSION

- The $CsYbCl_3$ crystals exhibit n-type semiconductors characteristics with broad optical absorption in the UV-vis-NIR region.
- The behaviors of electronic and thermal conductivities exhibit carrier scattering effect with lattice vibration in the high-temperature region.
- The optical and acoustic phonon originated from the distortion of crystal structure based on bond-interaction of p, d, f orbital in Yb and Cl.
- The photovoltaic characteristics will be improved by utilizing the crystal at cubic state with stable semi-conductivity over a wide temperature range.